Study on Shape-Memory Behavior of Polyether-Based Polyurethanes. I. Influence of the Hard-Segment Content

J. R. LIN,[1] L. W. CHEN[2]

[1] Institute of Materials Science and Engineering, National Taiwan University, Taipei, Taiwan, Republic of China

[2] Department of Chemical Engineering, National Taiwan University, Taipei, Taiwan, Republic of China

ABSTRACT: Shape-memory polyurethanes (PUs) were synthesized by 4,4′-diphenyl-methane diisocyanate (MDI), 1,4-butanediol (BD), and poly(tetramethyl oxide)glycol (PTMO). The morphology of PUs was studied using DSC, DMA, and TEM. The results indicated that the PUs would show different morphology by changing the mol ratio of MDI and BD (hard segment). The specimens would show the shape-memory behavior that was fixing and recovering the deformation at different operating temperature ranges. These results demonstrated that the shape-memory behavior of the PUs would be affected by the morphology and the modulus ratio that was defined as $E'_{T_g-20°C}/E'_{T_g+20°C}$ in DMA analysis. The amount of the hard-segment-rich phase would affect the ratio of recovery, that is, the low content would lead to the recovery of the deformed specimen being incomplete. The recovering rate would be influenced by the modulus ratio and the size of the dispersed phase in the micromorphology. On the other hand, the shape-memory behavior of PUs could be enhanced by the training process. © 1998 John Wiley & Sons, Inc. J Appl Polym Sci 69: 1563–1574, 1998

Key words: polyether-based polyurethanes; shape memory behavior; morphology; thermal properties; dynamic mechanical properties; hard segment

INTRODUCTION

A metallic alloy containing the same amounts of nickel and titanium was discovered that showed good shape-memory properties in the 1960s.[1] This investigation promoted the study of the shape-memory characteristic in the field of polymeric materials.[2–9] Polymeric materials which could fix the deformation without external force loading and recover the original shape after a series of thermomechanical treatments were named shape-memory polymers for the characteristics that they showed.[3] To perform the mechanical behavior of fixing and recovering the deformation, the mor-phology of shape-memory polymers should contain two phases, which were the reversible phase and the fixed phase.[4] The reversible phase showed a phase-transition temperature that was a little higher than the operating temperature. Therefore, the shape-memory polymers would be deformed if the reversible phase was heated to a softened state. When the reversible phase was cooled to a hardened state, it could fix the deformation. However, the fixed phase consisted of a high transition temperature or a crosslinking point. In the range of operating temperature, it was in the glassy state, the crystalline state, or the crosslinking point. Thus, the fixed phase could act as a rubber to recover the deformation.

For the different requirement of engineering design, the phase-transition temperature of the polymer depended on the practical application.

The elastomers were used at a temperature above the T_g for high mobility. The plastics were operated at temperature below the T_g because of their glasslike rigidity. However, the phase-transition temperature of the reversible phase in the shape-memory polymer was a little higher than the operating temperature.[3] When the reversible phase was heated to the softened state and treated under the external force, the shape of the polymers would change. Then, the deformed specimen was quenched to the hardened state. Because the strength of the hardened reversible phase was larger than the recovery force of the fixed phase, the deformation was "frozen" even if the external load was released. The deformation would not recover forever if the temperature was lower than the phase-transition temperature of the reversible phase. Once the hardened reversible phase was softened by heating to the temperature which was higher than the operating temperature, the factor of resisting the elastic recovery of the fixed phase disappeared, for example, the reversible phase was softened and the strength of it was reduced. Then, the specimen would recover the original shape because of the elastic recovery that was contributed by the fixed phase. Consequently, the shape-memory polymers showed the mechanical behavior that included fixing the deformation as the plastic and also recovering the deformation as the rubber. They behaved as plastic and rubber under a series of thermomechanical treatments. In such a manner, the shape-recovery function of the polymeric materials required the crosslinking or partial crystallization or glassy state in the molecular state. In addition, the fixed deformation function of the materials required the higher phase-transition temperature of the reversible phase in the operating temperature range.

Segmental polyurethanes (PUs) were composed of the flexible soft segment and the rigid hard segment. The former was based on the aliphatic polydiol, and the later, on the aromatic diisocyanate and the chain extender that was diol with the small molecular weight.[10,11] Repulsive interaction between the dissimilar segments[10] and the thermodynamical incompatibility[12] led to the phase separation and formed the hard- and soft-segment domains. The morphology of these domains affected the mechanical and thermal properties of the PUs. The chemical structure of the monomers, their composition, their stoichiometric ratio,[13–15] the sequence length distribution of the hard and soft segments,[16] overall molecular weight and its distribution, and the thermal history[17] could affect the morphology of the PUs.[18] By the investigation of the influence of the hard-segment content, Koberstein et al. proposed a morphological model which considered the length and distribution of the hard segment.[17,18] They described that the length of the hard segment which was shorter than a critical sequence length was dissolved in the soft-segment-rich phase. On the other hand, the longer hard segment would fold or coil to form the hard-segment-rich phase. Consequently, the aromatic diisocyanate and the chain extender formed the hard segment and the length distribution of the hard segment would lead to form the different morphology. Furthermore, the glass transition and the properties of PUs would be affected by the content of the hard segment.

As mentioned above, many kinds of shape-memory polymers were found. However, there were few reports to investigate the relationship between the morphology and the shape-memory behavior. In this study, the shape-memory PUs were expected to be synthesized. The PUs should show the optimized phase transition at the operating temperature range and compose two phases. For the purpose of studying the influence on the content of the hard segment, the PUs were synthesized with various mol ratios of MDI and BD. The morphology of the specimens were investigated using DSC and DMA. The morphologies of the PUs were directly observed by TEM with the stained technique. Finally, the PU with the optimum properties was chosen and its shape-memory behavior was tested by a bending test method.

EXPERIMENTAL

Materials

Reagent-grade poly(tetramethylene oxide)glycol (PTMO, MW = 650 and 250, Aldrich Chemical Co., Wisconsin, USA) and 1,4-butanediol (BD, Aldrich Chemical Co.) were dehydrated under a vacuum at 65°C before using. Reagent-grade 4,4′-diphenylmethane diisocyanate (MDI, Tokyo Chemical Inc., Tokyo, Japan) was melted at 45°C and used after removing the white precipitates in the melts. Reagent-grade N,N'-dimethylforamide (DMF, Aldrich Chemical Co.) was dehydrated with molecular sieves and used as a solvent.

Table I   Notation and Molar Compositions of the PUs

Notation	MDI/PTMO/BD Mol Ratio	Hard-segment Content (wt %)
PTMO250 series		
A1	1/1/0	56.8
A2	2/1/1	74.3
A3	3/1/2	81.7
A4	4/1/3	85.8
A6	6/1/5	90.2
A8	8/1/7	92.5
A10	10/1/9	93.9
A12	12/1/11	94.9
PTMO650 series		
B1	1/1/0	31.56
B2	2/1/1	50.33
B6	6/1/5	76.31
B8	8/1/7	81.22
B12	12/1/11	86.73

Polymer Synthesis

Four series of PUs of varying composition were synthesized with MDI, PTMO, and BD as the chain extender. To understand the influence of the content of the hard segment on the properties of the PUs, the mol ratios of MDI and BD were varied to synthesize the PUs with different contents of the hard segment. The compositions of the materials are listed in Table I. A modified two-step polymerization was adopted. The dehydrated MDI and PTMO were mixed at the mol ratio ($n : 1$) at 45°C and reacted at 65°C for 3 h. For the second step, the NCO-capped prepolymer was diluted with the DMF, and the dilute solution of BD in DMF was added slowly at 0°C. After mixing completely, the reaction system was heated to 65°C for 4 h. The reaction underwent a nitrogen gas atmosphere to avoid the influence of moisture during the synthesis process. The PU solution was cast onto a glass plate and kept at 65°C for 24 h. Finally, the PU film was immersed in purified water overnight. Then, the DMF was removed under a vacuum at 65°C for 24 h.

Polymer Characterization

Differential Scanning Calorimetry (DSC)

The thermal properties of PUs were measured by a DuPont 9900 thermal analyzer with a DSC mod-

ule, purged with nitrogen gas, and quenched with liquid nitrogen. The specimens were scanned from -150 to 250°C by a heating rate of 10°C per min. The cell was calibrated using an indium standard. The weight of the sample was 10–15 mg.

Dynamic Mechanical Analysis (DMA)

DMA measurements were carried out with a Du-Pont 983 DMA. Dynamic mechanical properties were measured in the tensile mode at a fixed frequency of 1 Hz and under nitrogen gas purging. A length-to-thickness ratio that was larger than 10 was used to negate the DMA's dependence on the Poisson ratio. The measured specimens were heated from -150 to 200°C using a heating rate of 5°C/min. The quantities of the storage modulus and loss modulus were recorded.

Transmission Electron Microscopy (TEM)

TEM images were observed on a TEM Hitachi H-600. The 400-mesh copper grids were immersed in a dilute PU solution and then the solvent was removed in a vacuum oven overnight. The cast copper grids were exposed on the vapor of the solution of RuO_4 at room temperature for 30 min and then washed with pure water and dried in the vacuum oven. Finally, the stained specimens were examined with TEM.

Shape-memory Behavior

The method of evaluating the shape-memory behavior of the shape-memory alloy[19] was adopted to investigate that of the PUs. The shape-memory behavior was examined by a bending test as follows: The specimen was deformed to an angle θ_i at 80°C and kept the deformation. The deformed specimen was quenched to -20°C and then the external force released. Finally, the deformed sample was heated to the test temperature (30–80°C) rapidly and the change of the angle θ_f with time was recorded. On the other hand, the deformed specimen was heated by a fixed heating rate and the relationship between the recoverable ratio and temperature was reported. The ratio of the recovery was defined as $(\theta_i - \theta_f)/\theta_i$. This process was designed as a temperature series test or a time series test hereafter.
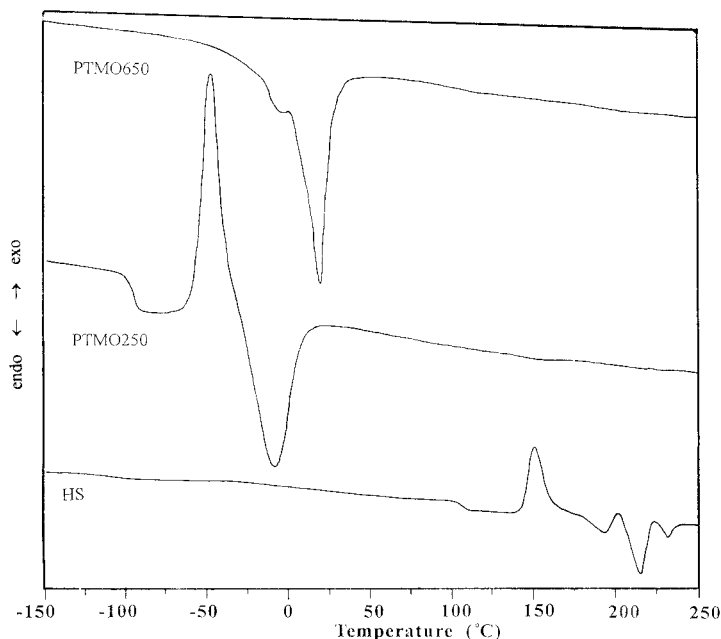
Figure 1 DSC scanning of pure soft-segment (PTMO250 and PTMO650) and pure hard segment (HS).

RESULTS AND DISCUSSION

Morphology of the PUs

Differential Scanning Calorimetry

All the thermal properties and characteristic temperatures such as the glass transition temperature (T_g), recrystallizing temperature (T_c), and crystal melting temperature (T_m) were measured using DSC and DMA. To reduce the influence of the thermal history,[10] all samples were heated to 250°C for 5 min. Then, these samples were cooled to −150°C quickly and then reheated to 250°C by a heating rate of 10°C/min.

The individual scanning results of the pure soft segment, PTMO, with various molecular weights and the pure hard segment (HS), which was MDI reacting with BD, are shown in Figure 1 and Table II. PTMO250 displayed glass transition behavior, recrystallization, and crystal melting step by step. However, PTMO650 only showed the crystal melting behavior in the range of temperature studied. The PTMO250 possessed more defects of the chain ends, so the crystal formation mechanism was disturbed. The pure hard segment (HS) showed high T_g's, T_c's, and T_m's for the aromatic structure. Therefore, the HS contained a glassy state and a crystal state.

The DSC curves of these series of PUs are dis-

played in Figures 2 and 3 and their thermal data are listed in Table II. The hard-segment domain of A1 could not form for lack of a chain extender, BD, and the thermal behavior of the hard segment was not observed.[12] In the spectrum of A2, MDI bonded with BD to form the hard segment, but it did not show the same thermal behavior as that of the HS. Therefore, it could be thought that most of the short hard segment were mixed with the soft segment.[15] A3, A4, and A6 displayed similar shapeliness of the DSC curves. The short hard segment of these samples had the same thermal behavior as that of A2. On the other hand, the long hard segment coagulated together and formed the hard-segment domains. Consequently, they showed glass transition, recrystallizing, and crystal melting behavior at high temperature as did the HS. The glass transition zone of the hard-segment domain overlapped that of the crystal melting of the short hard segment, so the T_g could not be observed easily. Because of the impediment from the short hard segment, the T_c's of A3, A4, and A6 were higher than that of the HS. The crystal of the long hard segment was not as perfect as that of the HS, so the T_m's of A3, A4, and A6 were lower than those of the HS and they displayed only one or two T_m's.

A8, A10, and A12 that contained more MDI and BD behaved as did the HS. These results implied

Table II   Heat Change Data of the Peak of the PUs

Sample	Crystallization ΔH (J/g)		Crystal Melting ΔH (J/g)	
	Soft-segment-rich Phase	Hard-segment-rich Phase	Soft-segment-rich Phase	Hard-segment-rich Phase
Pure soft segment				
PTMO 250	67.4	—[a]	74.4	—
PTMO 650	—	—	94.0	—
Pure HS				
HS	—	33.3	—	40.9
PTMO 250 series				
A1	—	—	—	—
A2	12.42	—	12.17	—
A3	19.56	8.27	15.18	20.60
A4	17.90	7.55	14.90	17.08
A6	24.23	10.70	15.44	27.93
A8	—	22.50	—	30.56
A10	—	24.33	—	37.36
A12	—	22.05	—	30.31
PTMO 650 series				
B1	—	—	—	—
B2	6.52	—	8.66	—
B6	—	17.19	—	19.41
B8	—	22.33	—	29.96
B12	—	24.76	—	29.84

[a] "—" indicates that the thermal behavior was not observed.

that the hard segment of these three samples were long enough to form a hard-segment-rich phase. Relatively, the amount of the short hard segment decreased and reduced the content of the mixing with the soft segment. Therefore, they did not easily show the thermal behavior as the above descriptions of the PUs with a low content of MDI and BD at the low temperature range. The T_g's, T_c's, and T_m's of A8, A10, and A12 would shift to a lower temperature than those of the HS for PTMO250.

The heat change of crystal melting was larger than that of recrystallizing as shown in Table II. This result implied that the PUs showed both crystalline and glassy states in the morphology. Hence, the A1 that was PTMO 250 reacted with MDI did not form the hard-segment phase. A2 was composed of the soft-segment-rich phase that was dissolved with the short hard segment, and another phase was some imperfect crystal of the

hard segment. A3, A4, and A6 comprised the soft-segment-rich phase as that of A2 and the hard-segment-rich phase that formed with the long hard segment. A8, A10, and 12A consisted of the hard-segment-rich phase that was an amorphous state and mixed with the PTMO250 and the crystal phase of the hard segment. Their soft-segment-rich phase was not detected in the DSC scanning.

Figure 3 displays the scanning results of the PUs which contained the soft segment of PTMO650 and the different mol ratios of MDI and BD. The DSC spectrum of B1 was similar to that of A1. The thermal behavior of B2 acted as that of A2, and B6, B8, and B12 showed the same thermal properties as those of A12.

Dynamic Mechanical Analysis

Figures 4 and 5 show the results of the DMA of the PUs and the data are listed in Table III. In
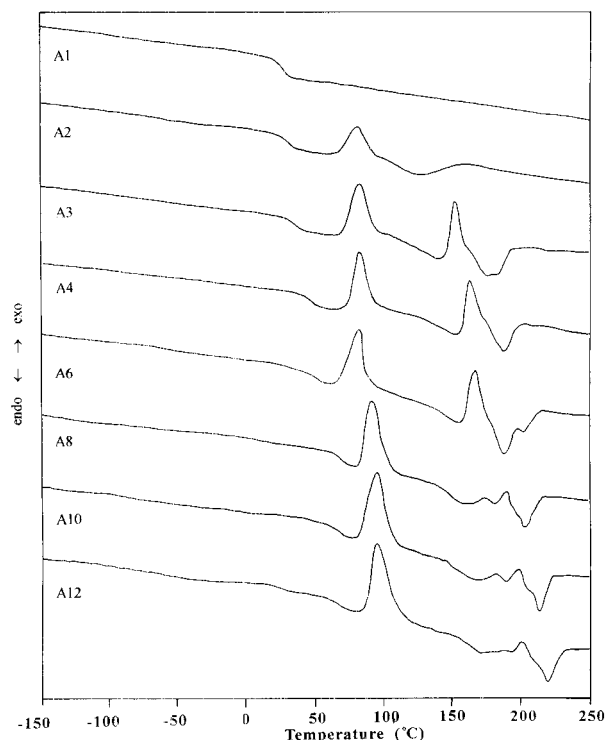
Figure 2 DSC scanning of the PTMO250 series.

Table III   DMA Data of the PUs

Sample	Glass Transition T_g (°C)	Storage Modulus Ratio[a]
A1	16.1	34.26
A2	17.1	14.74
A6	26.6	4.00
A12	54.1	3.87
B1	−13.4	139.64
B2	−8.1	18.41
B6	16.0	3.87
B12	38.4	3.87

[a] Storage modulus ratio was defined as $E'_{T_g-20°C}/E'_{T_g+20°C}$.[3]

served on the spectra of these specimens. Consequently, the compatibility of the soft segment and hard segment was better for increasing the mol ratio of MDI and BD. A similar comparison was found between the series of PTMO650. The modulus ratio that was defined as $E'_{T_g-20°C}/E'_{T_g+20°C}$ (ref. 3) decreased with an increasing mol ratio of MDI and BD, which Table III shows.

Transmission Electron Microscopy (TEM)

Figure 6 shows TEM micrographs of RuO_4-stained PUs. It successfully enhanced the image contrast for PUs using a staining technique; thus, the micro-morphology distribution of the specimen could be observed clearly. The TEM micrograph of the HS represented the pure hard segment; thus, it
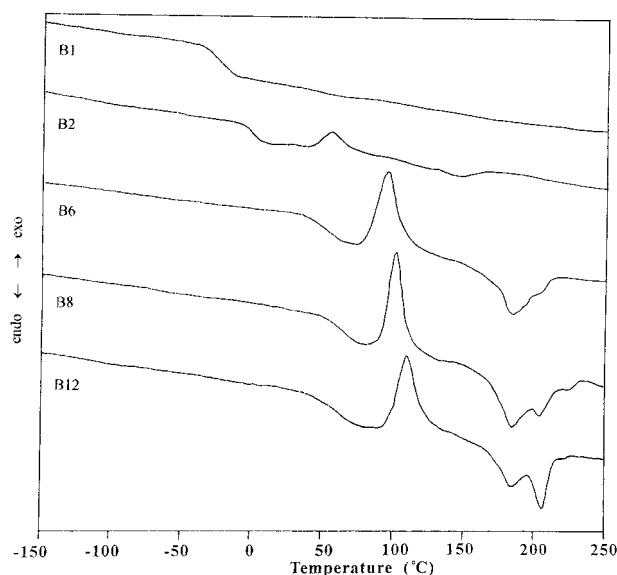
Figure 4, the dotted lines show the analysis results of the pure soft segment, PTMO250, and the dashed lines show those of the pure hard segment, HS. PTMO250 showed the glass transition at about −110°C and the storage modulus of it sharply decreased in the range of −50 to −25°C for the melting behavior. The T_g of the HS was 143°C and it would melt at a temperature that was higher than 200°C. So, the HS would showed steady mechanical properties at low temperature. The T_g of the specimen was indicated by the maximum value of the peak of the curves of the temperature-dependent loss modulus (E''). In the series of PUs that were based on PTMO250, the T_g's shifted to high temperature with increasing mol ratio of MDI and BD. The width of the peak was broadened for more hard-segment addition. The change of the tendencies of the curves of the temperature-dependent storage modulus (E') were shifted from the soft segment, PTMO250, to the hard segment, HS. Therefore, the softened temperature of the specimens would shift to that of the HS. On the other hand, the range of the glass transition was localized between the range of the glass transition of the soft segment and the hard segment. The individual transition peaks of the hard segment and the soft segment were not ob-

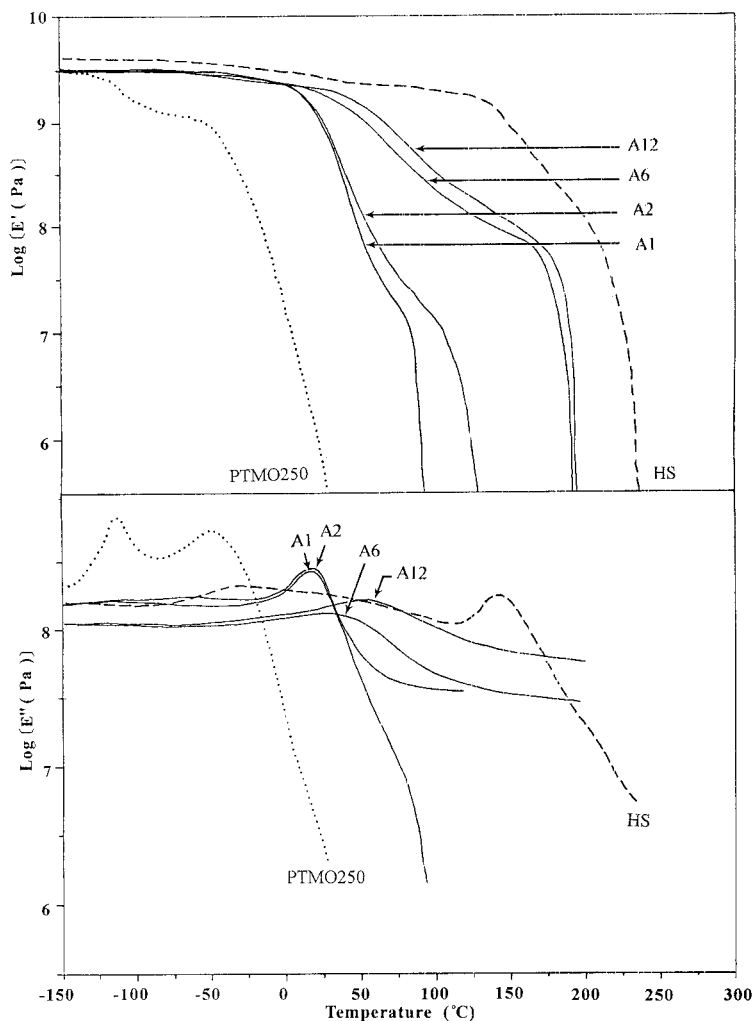**Figure 3** DSC scanning of the PTMO650 series.

Figure 4   DMA analysis of the (solid lines) PTMO250 series, (dotted line) PTMO250 and (dashed line) HS.

did not show a contrasted image. From the DSC analysis, the A2 contained two phases. One is the soft-segment-rich phase that is the short hard segment mixed with the soft segment. The other is the crystal hard-segment phase that was in the crystalline state. Therefore, the TEM micrograph of A2 displayed the contrast pattern. In the micrograph, the hard segment was the continuous phase which had a network structure, and the soft-segment-rich phase was the dispersed phase with an average diameter about 30–50 nm. The micromorphology of A12 was similar to that of A2. However, the average size of the dispersed phase was smaller than that of A2. There was a greater ratio of the hard segment in A12 and it almost formed the hard-segment domain. Therefore, the amount of the short hard segment that mixed

with the soft segment was reduced as described in the DSC analysis. The dispersed phase was smaller and more uniform in the morphology of A12 than that of A2, that is, the compatibility of these two phases of A12 was much better than that of A2. This result was consistent with the conclusion of the DMA.

Shape-memory Behavior

Temperature Series Study

The shape-memory behavior of PUs based on the different mol ratios of MDI and BD was detected in the temperature series study as shown in Figure 7. In Figure 7, the reversible ratio of the specimens was less than 10% at the low-temperature range
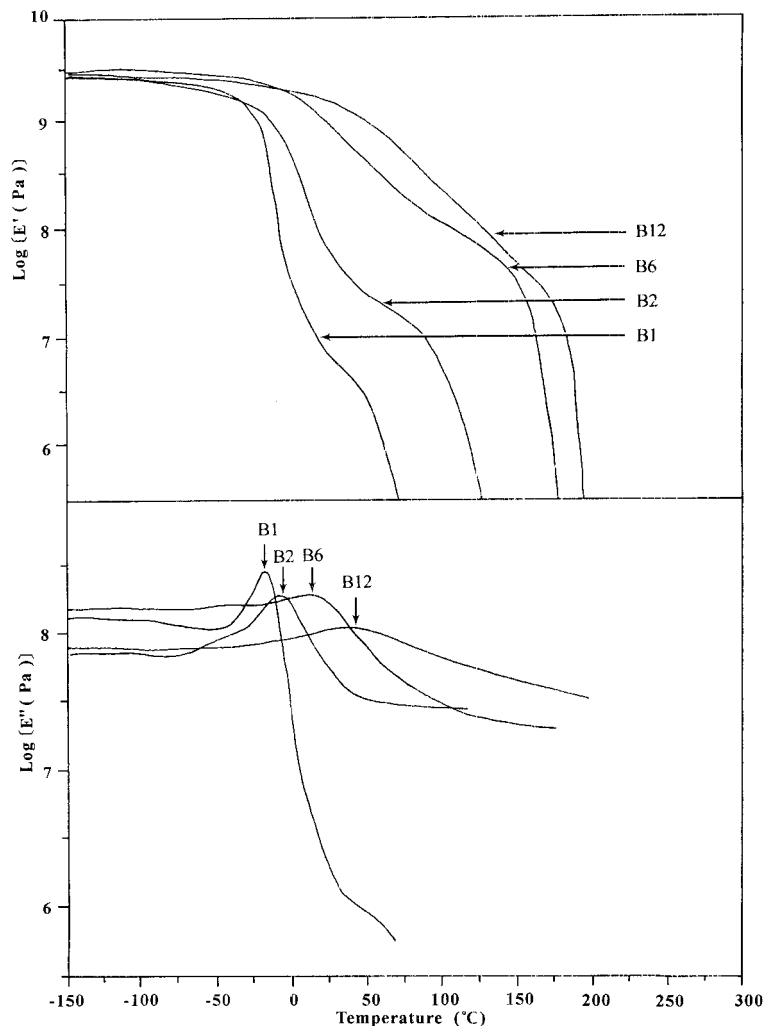
Figure 5   DMA analysis of the PTMO650 series.

(−20 to 0°C). The deformed A1 would recover the deformation rapidly when it was heated to high temperature. However, it could not recover to the original shape, that is, there was residual deformation that could not recover under the testing process. A2 would recover the deformation at a higher temperature range than A1 showed, but the recovering rate of A2 was slower than that of A1. In addition, A2 would completely recover to the original shape and did not show the residual deformation. A6 showed a higher-temperature range for recovering and a slower recovering rate than those of A2. The same comparison was found between A6 and A12. A6 and A12 also showed 100% recovery.

By the temperature series study, the shape-memory behavior of PUs was found. They would keep the deformation at the temperature range which was lower than the T_g of them and recover to the original shape under the heating process. In the morphological investigation of DSC, DMA, and TEM, the PUs based on the different compositions showed different morphology, modulus ratio, and particle size of the dispersed phase. The recovering rate of them would be fast with a high storage modulus ratio, that is, the PUs could show better shape-memory behavior when their storage modulus ratio was high. Consequently, A1, with a high modulus ratio, showed a better behavior of deformation recovery than did the others. The recovery rate would be slow when the mol ratio of MDI and BD was increased from A1 to A12, whose modulus ratio also was reduced gradually. However, the deformed A1 would not recover completely because the morphology of it only just showed the soft-segment phase that reacted with MDI and the behavior of the hard segment was
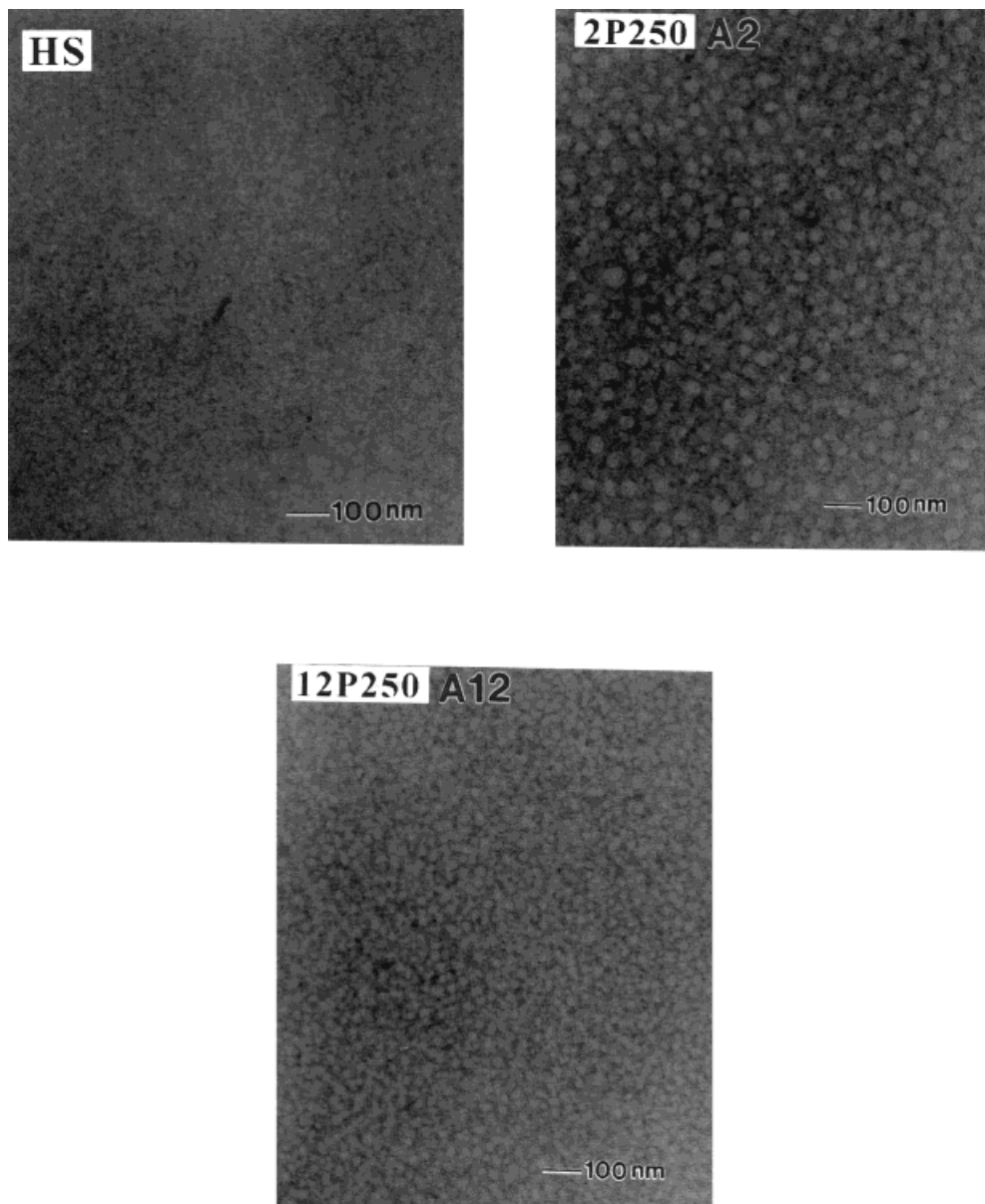
Figure 6 TEM micrographs of the PTMO250 series: A2(2P250); A12(12P250); HS (×60,000).

not found. Hence, it did not possess enough elastic force to recover the deformation completely. A12 could recover to original shape for containing enough hard segment content. As shown in the morphology study, the compatibility of A12 was better than that of the others and led to the low storage modulus ratio. Therefore, the sensitivity of the shape memory of A12 which depended on temperature was slower than that of A1 in the shape-memory behavior testing.

As the study above showed, the shape-memory behavior of PUs would be influenced by the modulus ratio and their morphology. In the shape-recovering process, the PUs that showed a high modulus ratio would display a fast shape-recovery rate. However, the morphology of their hard-segment-rich phase would affect the ratio of recovery. As mentioned above, the morphology of the shape-memory polymer contained two phases: One was the reversible phase whose transition temperature must be higher than the operating temperature in order to fix the deformation. On the other
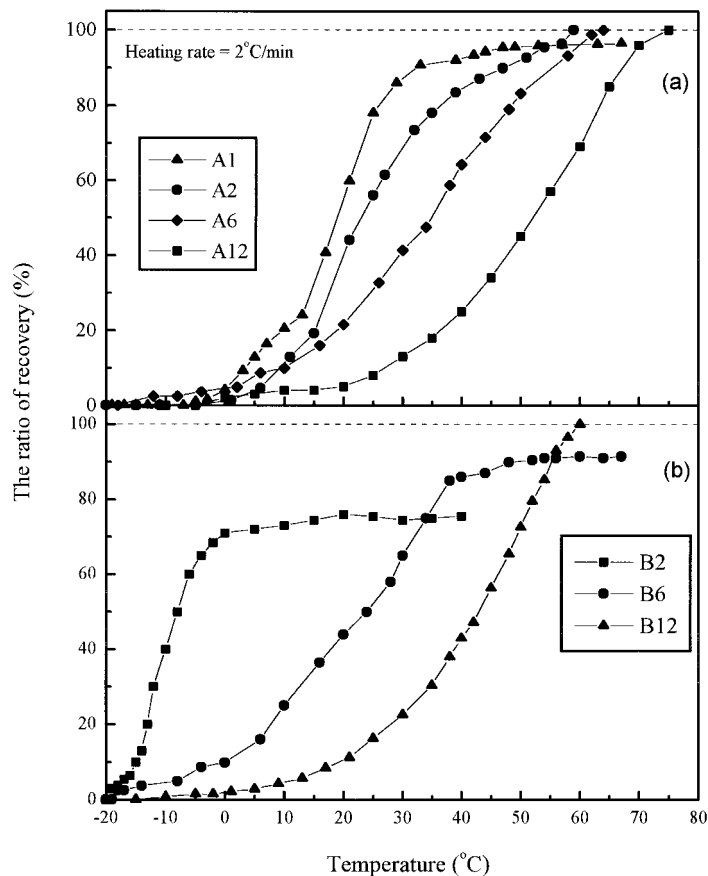
Figure 7 Shape-memory behavior of these series in the temperature series study: (a) PTMO250; (b) PTMO650.

hand, the characteristic temperature of the fixed phase should be higher than that of the reversible phase and operating temperature. The fixed phase could execute the work to recover the deformation. Therefore, the hard-segment-rich phase of the PUs showed the same behavior of the fixed phase of the shape-memory polymers. The soft-segment-rich phase of A1, A2, and A6 or the amorphous state of A12 would show the same behavior of the reversible phase of the shape-memory polymers.

Time Series Study

The influence of the content of the hard segment on the glass transition temperature of PUs was investigated by DSC and DMA. The T_g would shift to high temperature when the mol ratio of MDI and BD increased. Consequently, the A12 whose T_g was 54.1°C was selected to understand the shape-memory behavior in the time series study. The PTMO250 mixed with the hard segment rep-

resented the reversible phase and the crystal hard segment acted as the fixed phase. Figure 8 displays the relationship between the ratio of recovery and time under different testing temperatures. The deformation would quickly recover at the temperature that was higher than the T_g of A12. The deformation only recovered partially and kept the deformation during the testing period at the testing temperature of 30 and 40°C. This conclusion was consistent with the result of the temperature series study. The deformed specimen would recover the original shape gradually if the temperature was increased to the temperature range of 50–80°C). Figure 9 showed the results of the influence of the number of testings on the ratio of recovery. The ratio of recovery would be reduced and approximated a steady value as the number of testings increased. If the recoverable ratio of the 99th testing was compared with the result of the 100th testing, the relative ratio of recovery would approach 100%. Consequently,

A12 could show better shape-memory behavior after the process of training.

CONCLUSION

The morphological investigation of the shape-memorized PUs was done using DSC, DMA, and TEM. The change of morphology between the soft-segment domain and hard-segment domain of the PUs depended on the content of the hard segment (MDI + BD). The greater amount of MDI and BD used, (i) the higher the T_g and (ii) the lower the modulus ratio of the PUs obtained. The compatibility between the soft-segment domain and the hard-segment domain would be better when the content of the hard segment was increased, as indicated by the DMA and TEM data. The results also indicated that the reversible phase of shape-
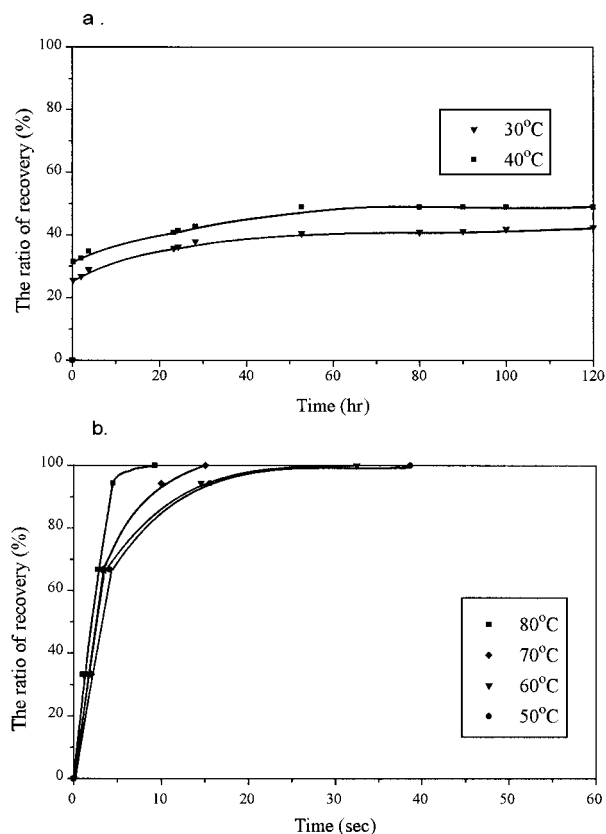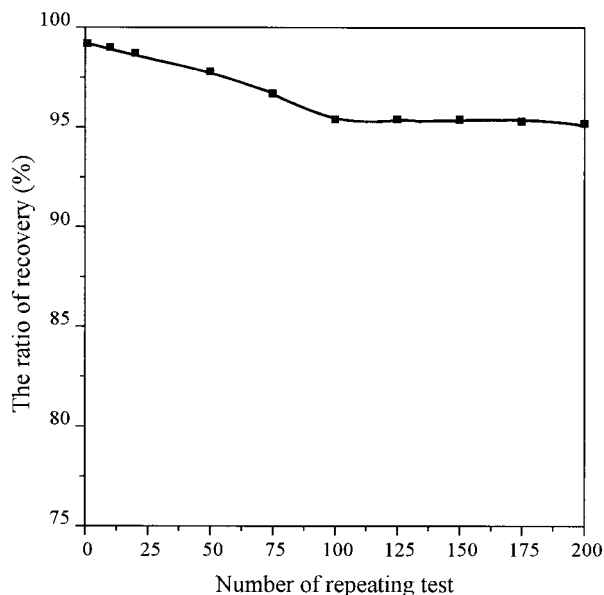
Figure 9 Relationship between the ratio of recovery and numbers of the testing of A12.

memorized PUs was the soft-segment-rich phase containing PTMO and the short hard segment. The fixed phase was the hard-segment-rich phase. Shape-memorized PUs with high T_g's would show a high recovery temperature. They would show better shape-memory behavior with a higher modulus ratio than with a lower modulus ratio. On the other hand, the ability of shape-memory PUs would be enhanced after a thermal training series.

Figure 8 Shape-memory behavior of A12 in time series study: (a) test temperature was lower than the T_g of A12; (b) test temperature was higher than the T_g of A12.

REFERENCES

1. H. Funakuba, *Shape Memory Alloys,* Vol. 1, Gordon and Breach Science Publisher, New York, Chap. 3 (1987).
2. K. Nakyama, *Int. Polym. Sci. Technol.,* **18**(3), 43 (1991).
3. S. Hayashi, *Int. Prog. Urethane,* **6,** 90 (1993).
4. M. Ishii, *Plast. Age,* **15**(6), 158 (1989).
5. S. Hayashi, S. Kondo, P. Kapadia, and E. Ushioda, *Plast. Eng.,* **51**(2), 29 (1995).
6. H. Tobushi, S. Hayashi, and S. Kojima, *JSME Int. J. Ser. 1,* **35,** 296 (1992).
7. K. Takeda, M. Ayiyama, and T. Yamamizu, *Angew. Macromol. Chem.,* **157,** 123 (1988).
8. T. Shiga and T. Kurauchi, *J. Appl. Polym. Sci.,* **39,** 2308 (1989).

9. T. Hirai, H. Maruyama, T. Suzuki, and S. Hayashi, *J. Appl. Polym. Sci.,* **45,** 1849 (1992).

10. R. J. Zdrahala, R. M. Gerkin, S. L. Hager, and F. E. Critchfield, *J. Appl. Polym. Sci.,* **24,** 2041 (1979).

11. K. C. Frish and S. L. Reegen, *Adv. Urethane Sci. Technol.,* **2,** 29 (1973).

12. H. K. Lee and S. W. Ko, *J. Appl. Polym. Sci.,* **50,** 1269 (1993).

13. G. Spathis, M. Niaounakis, E. Kontou, L. Apekis, P. Pissis, and C. Christodoulides, *J. Appl. Polym. Sci.,* **50,** 831 (1994).

14. R. P. Redman, in *Developments in Polyurethanes,* J. M. Buist, Ed., Applied Science, London, 1978, Chap. 3.

15. R. F. Harris, M. D. Joseph, C. Davidson, C. D. Deporter, and V. A. Dais, *J. Appl. Polym. Sci.,* **41,** 509 (1990).

16. L. M. Leung and J. T. Koberstein, *Macromolecules,* **19,** 706 (1986).

17. J. T. Koberstein and R. S. Stein, *J. Polym. Sci. Polym. Phys.,* **21,** 1439 (1983).

18. W. Hu and J. T. Koberstein, *J. Polym. Sci. Polym. Phys.,* **32,** 437 (1994).

19. H. C. Lin and S. K. Wu, *Scr. Met.,* **26,** 959 (1992).